

AN EFFICIENT APPROACH TO UNSUPERVISED OUT-OF-DISTRIBUTION DETECTION WITH VARIATIONAL AUTOENCODERS

Zezhen Zeng, Bin Liu*

Research Center for Applied Mathematics and Machine Intelligence, Zhejiang Lab
Hangzhou 311121, China

ABSTRACT

This paper is concerned with deep generative models (DGMs) for unsupervised out-of-distribution (OOD) detection. In particular, we focus on vanilla Variational Autoencoders (VAE) that use a standard normal prior distribution for the latent variables. These models have a smaller model size, enabling faster training and inference, making them well-suited for resource-limited applications compared to more complex DGMs. We propose a novel OOD score called Error Reduction (ER) specifically designed for vanilla VAE. ER incorporate the idea of reconstructing image inputs from their lossy counterparts and takes into account the Kolmogorov complexity of the images. Experimental results on diverse datasets demonstrate the superiority of our approach over baseline methods. Our code is available at: <https://github.com/ZJLAB-AMMI/VAE4OOD>.

Index Terms— out-of-distribution, variational autoencoder, Kolmogorov complexity, unsupervised

1. INTRODUCTION

The reliability of deep learning models in real-world applications is crucial for modern society. One essential aspect of ensuring model reliability is the ability to differentiate between in-distribution (ID) data and out-of-distribution (OOD) data. While many studies have focused on supervised OOD detection [1, 2, 3, 4], real-world applications often require efficient unsupervised approaches, as data labels are frequently unavailable. Deep generative models (DGMs) are commonly employed for unsupervised OOD detection. In this paper, we specifically concentrate on a well-known DGM, namely Variational Autoencoders (VAEs). These VAEs possess a smaller model size, allowing for faster training and inference. This attribute makes them highly suitable for real-world applications where efficiency is crucial.

A well-trained generative model is expected to assign higher likelihoods to ID samples and lower likelihoods to OOD ones, as the latter originate from distributions that differ from the distribution of ID samples [5]. However, several studies have shown that in practice, DGMs often assign higher

likelihoods to OOD samples than to ID samples [6]. This counterintuitive phenomenon has sparked a series of studies aimed at understanding and resolving the issue of likelihood misalignment [7, 8, 9, 10], which proposed new OOD scores to replace likelihood. Such scores still struggle to work with vanilla VAEs [11]. An alternative approach to address likelihood misalignment is to utilize more complex model structures, such as PixelCNN [12] and Glow [13]. Compared to these models, vanilla VAEs are preferable for resource-constrained scenarios due to their lightweight nature, faster training, and model inference. This motivates us to design a competent OOD score specifically tailored for vanilla VAEs, enabling reliable and highly efficient unsupervised OOD detection.

In this paper, we propose a novel OOD score called Error Reduction (ER) for vanilla VAEs. Our experimental results demonstrate that using the ER score effectively addresses the issue of likelihood misalignment and achieves reliable OOD detection without compromising the inference efficiency associated with vanilla VAEs.

2. BACKGROUND AND RELATED WORK

Assuming that $\mathbf{X} = \{\mathbf{x}_i\}_{i=1}^N$ represents a set of N independently and identically distributed (i.i.d.) samples drawn from an in-distribution $\mathbf{x} \sim p(\mathbf{x})$, the objective is to determine whether an unseen sample belongs to the in-distribution or not. A generative model trained on \mathbf{X} is expected to learn a good approximation of the underlying distribution $p(\mathbf{x})$. Consequently, OOD samples should be assigned lower likelihood scores by a well-trained generative model. However, in practical scenarios, OOD samples might receive higher likelihood scores than ID ones [6].

To address the aforementioned issue of likelihood misalignment, Ren *et al.* [7] propose a model for learning background information. Serra *et al.* find that input complexity significantly affects the likelihoods of generative models, leading them to propose a novel likelihood score regularized by an estimate of input complexity [8]. However, when applied to VAEs, these methods perform unsatisfactorily, as detailed in the experiment section, particularly in Table 1.

Likelihood Ration (LR) is a VAE-based method that achieves a high detection accuracy, albeit with a compromise

*Address correspondence to bins@ieee.org. This work was supported by Exploratory Research Project (No.2022RC0AN02) of Zhejiang Lab.

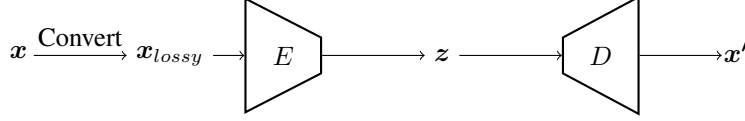


Fig. 1: The training scheme of our approach. x_{lossy} denotes a lossy counterpart of x . E and D represent the encoder and decoder respectively. z is the latent variable, and x' represents the reconstruction of x .

on inference efficiency, as it requires iterative optimization of the encoder for each test sample [9]. Floto *et al.* [10] propose a tilted Gaussian prior VAE to improve OOD detection, while Cai *et al.* [14] introduce an additional channel for high-frequency features during training.

3. OUR APPROACH

Here we present our approach built upon the vanilla VAE to unsupervised OOD detection using a newly proposed OOD score termed ER. The training scheme of our approach is depicted in Fig. 1. Given a set of ID samples, the first step is to perform a lossy operation on each sample, denoted as x , to obtain its lossy counterpart, denoted as x_{lossy} . This lossy operation reduces the input’s complexity while retaining essential information. Next, we train a VAE model using the ID samples and their corresponding lossy counterparts. The VAE learns to reconstruct the original samples from their lossy counterparts. During the test stage, we apply the same lossy operation to each test sample. Then, we use the trained VAE model to generate a reconstructed image from the lossy sample. Finally, we calculate the ER score, and a larger score value suggests that the test sample is an ID sample.

The ER score of an test image x is defined as follows

$$ER(x) = E(x, x_{lossy}, x') + \underbrace{\lambda(L(x) - L(x_{lossy}))}_{\text{regularisation term}}, \quad (1)$$

where $E(x, x_{lossy}, x') \triangleq d(x, x_{lossy}) - d(x, x')$ quantifies the discrepancy between two distances. The first distance $d(x, x_{lossy})$ measures how much information is lost during the lossy operation and the other distance, namely $d(x, x')$, measures how well the VAE model is able to reconstruct the original input. In the regularisation term, $L(\cdot)$ denotes an estimate of the Kolmogorov complexity [15], a measure of the amount of information required to describe an object. This regularisation term helps consider the complexity of the input sample in the ER score calculation. The hyper-parameter λ controls the weight given to the input complexity component in the ER score. When λ is set at 0, then $ER(x) = E(x, x_{lossy}, x')$. We conducted experiments to investigate various choices for the lossy operation, the distance function d , and the λ values. See details in subsection 4.3.

3.1. Why the ER score works?

Consider an ID sample x and an OOD sample y to be tested. For the ID sample x , if the VAE model is trained sufficiently well on the ID data, the lossy operation primarily affects the quality of its latent code z . However, it does not significantly impact the quality of the reconstructed sample. This is because the VAE can still effectively learn to “autoencode” the data by utilizing an expressive decoding distribution $p(x|z)$ [16]. The decoder is optimized to ignore the latent code z and focus on reconstructing the input.

Based on the above observation, we can infer that the dissimilarity measure $d(y, y')$ should be significantly larger than $d(x, x')$, as y' is obtained by a model trained to reconstruct ID data rather than OOD samples like y . Therefore, assuming that $d(y, y_{lossy})$ is not excessively larger than $d(x, x_{lossy})$, it is likely that $E(x, x_{lossy}, x')$ will be much larger than $E(y, y_{lossy}, y')$. However, if $d(y, y_{lossy})$ becomes so large compared to $d(x, x_{lossy})$ that $E(y, y_{lossy}, y')$ surpasses $E(x, x_{lossy}, x')$, using function E separately, namely setting λ in Eqn.(1) to 0, would fail to detect the OOD sample.

Now, let us consider when the value of $d(y, y_{lossy})$ becomes unexpectedly large. As the lossy operation reduces the diversity of pixel values in the image y and causes many pixel values of y_{lossy} to cluster within a specific range, a large value of $d(y, y_{lossy})$ occurs when the pixel values in y consistently deviate from that range. Such a consistency results in a low Kolmogorov complexity. An extreme example is when all pixels in y take on either the maximum or minimum value, which corresponds to the lowest complexity. This connection between $d(y, y_{lossy})$ and y ’s complexity motivates us to consider the Kolmogorov complexity in the design of our ER score. By incorporating the Kolmogorov complexity, as shown in Eqn.(1), we anticipate a smaller ER score for an OOD sample y that exhibits an unexpectedly large value of $d(y, y_{lossy})$.

In our experiments, we estimate the Kolmogorov complexity of an image using a Portable Network Graphics (PNG)-based image compressor in the same way as in [8].

4. EXPERIMENTS

4.1. Experimental setting

We validate our method using a widely used ID/OOD dataset pair: CIFAR10[17]/SVHN[18]. In addition, we assess the effectiveness and efficiency of our approach on various additional OOD datasets: FashionMNIST[19], MNIST[20],

	LR[9]	LL [11]	IC [8]	FRL [14]	LRatio[7]	Tilt [10]	Tilt + WIM[10]	ER (ours)
ID dataset: CIFAR10								
MNIST	0.986	0	0.976	0.984	0.032	0.797	0.941	0.987
FMNIST	0.976	0.032	0.987	0.993	0.335	0.688	0.939	0.984
SVHN	0.912	0.209	0.938	0.854	0.732	0.143	0.787	0.954
LSUN	0.606	0.833	0.348	0.449	0.508	0.933	0.650	0.654
CelebA	0.738	0.676	0.310	0.608	0.404	0.877	0.846	0.621
Noise	0.994	1	0.042	0.925	0.851	1	0.797	1
Constant	0.974	0.015	1	1	0.902	0	1	1
Average	0.885	0.395	0.657	0.830	0.538	0.634	0.851	0.886
Images/s	1.2	268.8	245.1	227.9	190.1	295.9	13.8	186.9
ID dataset: CelebA								
iNaturalist	0.808	0.993	0.955	0.995	0.969	0.845	0.650	0.985
Places	0.928	0.933	0.976	0.991	0.847	0.922	0.734	0.993
SUN	0.929	0.945	0.959	0.987	0.884	0.953	0.764	0.995
Textures	0.842	0.938	0.918	0.965	0.891	0.775	0.606	0.970
Average	0.877	0.952	0.952	0.984	0.898	0.874	0.689	0.986
Images/s	0.8	108.7	51.0	31.4	69.4	158.7	8.4	23.3

Table 1: AUROC results of ER and other VAE-based OOD detection methods. The last row of each table shows the number of images that each method can process per second. A larger value of this metric indicates better inference efficiency. The best result is marked in **bold**.

KMNIST[21], CelebA[22], LSUN[23], as well as two synthetic datasets, Noise and Constant, as reported in [9]. All images are resized to 32x32 pixels. Furthermore, we replicate the experimental setup described in FRL[14] and evaluate our method on high-resolution datasets: iNaturalist[24], Places[25], SUN[26], and Textures[27]. For these datasets, all images are resized to 128x128 pixels. We primarily base the architecture of our VAE on Floto et al.[10]. To measure the performance of OOD detection, we employ the Area Under the Receiver Operator Characteristic (AUROC) metric. A lower AUROC value indicates better performance in detecting OOD samples.

4.2. Experimental Results

Performance comparison on commonly used benchmark datasets We conducted a comparative analysis of our approach with several related VAE-based methods [11, 7, 8, 9, 10, 14]. In our experiments, we utilized nearest neighbor interpolation with a scale factor of 4 as the lossy function to generate the lossy counterparts of input images. The results are presented in Table 1. Note that the original implementation of the Tilt + WIM method [10] requires access to batches of OOD samples for network optimization. However, obtaining batches of OOD samples in advance may not be feasible in many real-world applications. To simulate such scenarios, we implemented the

Tilt + WIM method based on their released code, but replaced batches of OOD samples with a single OOD sample to be tested, following the same approach used for implementing the LR method [9].

As shown in Table 1, our proposed ER method achieves the highest average AUROC values across all datasets. Notably, ER does not require fine-tuning the encoder for each test sample, resulting in reduced processing time compared to LR [9]. Our experiments were conducted on a Tesla V100 GPU server, and ER demonstrates faster execution without compromising competitive performance.

FRL is another method that exhibits fast processing times while maintaining a satisfactory level of performance. However, the average AUROC value of FRL is lower than that of ER. Furthermore, when compared to the IC method [8], ER demonstrates a significant improvement in performance.

Performance comparison on high-resolution datasets Following the experimental setting of [14], we evaluated the effectiveness of our approach on high-resolution datasets, with CelebA being the ID dataset. The results of these experiments are presented in Table 1. In this case, we employed a scale factor of 8 for nearest neighbor interpolation.

As shown in the table, ER achieves the best average performance on high-resolution datasets, while FRL is the second-best method. However, considering processing time, FRL

	Nearest	Bilinear	75% Mask	$\beta = 10$
Average	0.886	0.696	0.865	0.821

Table 2: Averaged AUROC number corresponding to different lossy operations. The ID dataset is CIFAR10.

	S = 2	S = 4	S = 8	S = 16
Average	0.844	0.886	0.846	0.780

Table 3: Averaged AUROC results of our approach when using the nearest neighbor interpolation as the lossy operation. Different scale factor values of this operation are considered and compared here. The ID dataset is CIFAR10.

exhibits faster execution compared to ER. It is worth noting that the processing time of methods related to input complexity decreases more than other methods due to the additional time required for compressing larger images.

Both the Tilt + WIM and LR methods show less effectiveness on high-resolution datasets. We hypothesize that these two methods may require longer optimization iterations for larger image sizes, resulting in increased processing time.

4.3. Ablation Studys

On the lossy operation We explored four lossy operations to obtain the lossy counterpart of an image: nearest neighbor interpolation, bilinear interpolation with a scale factor of 4, patch masking, and image reconstruction with β -VAE [28]. We determined the hyperparameters for the masking operation and β -VAE that yielded the best results. Specifically, for the former, the masking ratio is set at 75%, and for the latter, β is set to 10. As shown in Table 2, the nearest neighbor interpolation achieved the best performance among these methods. Additionally, we investigated the impact of the scale factor involved in the nearest neighbor interpolation operation. This factor controls the degree of information loss. The results are summarized in Table 3, where it can be observed that the best performance was obtained at a scale factor of 4, and a significant drop in performance occurred when it was set to 16. Based on these findings, we recommend using nearest neighbor interpolation as the preferred lossy function while ensuring that the level of information loss is controlled appropriately.

On the distance metric In calculating the ER score, as defined in Eqn. (1), we explored multiple choices for the distance metric d , including cross-entropy (CE), mean absolute error (MAE), mean squared error (MSE), and LPIPS [29]. The results presented in Table 4 indicate that CE performs the best among these metrics. Additionally, MAE and MSE yield comparable performance to CE. However, LPIPS significantly

underperforms compared to the other metrics. Based on these findings, we recommend utilizing CE as the preferred distance metric for calculating the ER score, while also considering MAE or MSE as viable alternatives.

	CE	MAE	MSE	LPIPS
Average	0.886	0.855	0.836	0.507

Table 4: Average AUROC results of our approach corresponding to different distance metrics for d in Eqn.(1). The ID dataset is CIFAR10.

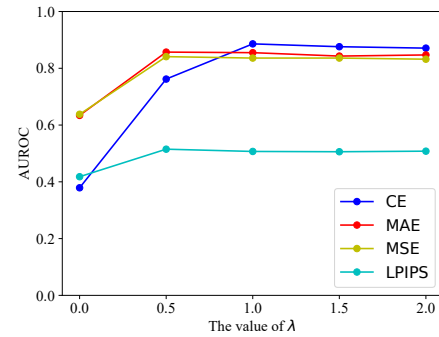


Fig. 2: The average AUROC results for different λ values with different distance metrics when the ID dataset is CIFAR10.

On the λ value We examined the impact of the parameter λ in Eqn.(1) on the performance of the ER score. As illustrated in Fig. 2, we observed that for all distance metrics, the performance stabilizes when λ takes a value between 1 and 2. This suggests that setting λ to a value between 1 and 2 leads to stable and reliable ER score performance.

5. CONCLUSIONS

In this paper, we presented a novel approach to tackle the challenging problem of unsupervised OOD detection. Our approach is characterized by two key components: the use of a lightweight vanilla VAE model architecture and the introduction of novel OOD score called ER. Through extensive experimentation and evaluation, we demonstrated that our approach offers a promising solution to the problem of unsupervised OOD detection, providing both high detection accuracy and inference efficiency.

Although ER is designed within the traditional VAE framework, it can be extended to more advanced DGMs such as the denoising diffusion implicit model [30], albeit with a compromise on inference efficiency. However, exploring this possibility is beyond the scope of this study and is left as a topic for future research.

6. REFERENCES

- [1] D. Hendrycks and K. Gimpel, “A baseline for detecting misclassified and out-of-distribution examples in neural networks,” in *ICLR*, 2016. 1
- [2] B. Lakshminarayanan, A. Pritzel, and C. Blundell, “Simple and scalable predictive uncertainty estimation using deep ensembles,” in *NeurIPS*, 2017. 1
- [3] S. Liang, Y. Li, and R. Srikant, “Enhancing the reliability of out-of-distribution image detection in neural networks,” in *ICLR*, 2018. 1
- [4] Y. Hsu, Y. Shen, H. Jin, and Z. Kira, “Generalized ODIN: Detecting out-of-distribution image without learning from out-of-distribution data,” in *CVPR*, 2020, pp. 10951–10960. 1
- [5] C. M. Bishop, “Novelty detection and neural network validation,” *IEEE Proceedings-Vision, Image and Signal processing*, vol. 141, no. 4, pp. 217–222, 1994. 1
- [6] E. Nalisnick, A. Matsukawa, Y. W. Teh, D. Gorur, and B. Lakshminarayanan, “Do deep generative models know what they don’t know?,” in *ICLR*, 2019. 1
- [7] J. Ren, P. J. Liu, E. Fertig, J. Snoek, R. Poplin, M. Depristo, J. Dillon, and B. Lakshminarayanan, “Likelihood ratios for out-of-distribution detection,” in *NeurIPS*, 2019. 1, 3
- [8] J. Serrà, D. Álvarez, V. Gómez, O. Slizovskaia, J. Núñez, and J. Luque, “Input complexity and out-of-distribution detection with likelihood-based generative models,” in *ICLR*, 2020. 1, 2, 3
- [9] Z. Xiao, Q. Yan, and Y. Amit, “Likelihood regret: An out-of-distribution detection score for variational auto-encoder,” in *NeurIPS*, 2020. 1, 2, 3
- [10] G. Floto, S. Kremer, and M. Nica, “The tilted variational autoencoder: Improving out-of-distribution detection,” in *ICLR*, 2023. 1, 2, 3
- [11] D. P. Kingma and M. Welling, “Auto-encoding variational Bayes,” in *ICLR*, 2013. 1, 3
- [12] T. Salimans, A. Karpathy, X. Chen, and D. P. Kingma, “Pixelcnn++: Improving the pixelcnn with discretized logistic mixture likelihood and other modifications,” in *ICLR*, 2017. 1
- [13] D. P. Kingma and P. Dhariwal, “Glow: Generative flow with invertible 1x1 convolutions,” in *NeurIPS*, 2018, vol. 31. 1
- [14] M. Cai and Y. Li, “Out-of-distribution detection via frequency-regularized generative models,” in *WACV*, 2023, pp. 5521–5530. 2, 3
- [15] A. N. Kolmogorov, “On tables of random numbers,” *Sankhyā: The Indian Journal of Statistics, Series A*, pp. 369–376, 1963. 2
- [16] X. Chen, D. P. Kingma, T. Salimans, Y. Duan, P. Dhariwal, J. Schulman, I. Sutskever, and P. Abbeel, “Variational lossy autoencoder,” in *ICLR*, 2017. 2
- [17] A. Krizhevsky and G. Hinton, “Learning multiple layers of features from tiny images,” 2009. 2
- [18] Y. Netzer, T. Wang, A. Coates, A. Bissacco, B. Wu, and A. Ng, “Reading digits in natural images with unsupervised feature learning,” 2011. 2
- [19] H. Xiao, K. Rasul, and R. Vollgraf, “Fashion-mnist: a novel image dataset for benchmarking machine learning algorithms,” *arXiv preprint arXiv:1708.07747*, 2017. 2
- [20] Y. LeCun, “The MNIST database of handwritten digits,” <http://yann.lecun.com/exdb/mnist/>, 1998. 2
- [21] T. Clanuwat, M. Bober-Irizar, A. Kitamoto, A. Lamb, K. Yamamoto, and D. Ha, “Deep learning for classical Japanese literature,” *arXiv preprint arXiv:1812.01718*, 2018. 3
- [22] Ziwei L., “Deep learning face attributes in the wild,” in *ICCV*, 2015. 3
- [23] Fisher Y., “Lsun: Construction of a large-scale image dataset using deep learning with humans in the loop,” *arXiv preprint arXiv:1506.03365*, 2015. 3
- [24] Van H., “The iNaturalist species classification and detection dataset,” in *CVPR*, 2018, pp. 8769–8778. 3
- [25] Bolei Z., “Places: A 10 million image database for scene recognition,” *IEEE Trans. on PAMI*, 2017. 3
- [26] J. Xiao, “Sun database: Large-scale scene recognition from abbey to zoo,” in *CVPR*, 2010, pp. 3485–3492. 3
- [27] M. Cimpoi, “Describing textures in the wild,” in *CVPR*, 2014. 3
- [28] I. Higgins, L. Matthey, A. Pal, C. Burgess, X. Glorot, M. Botvinick, S. Mohamed, and A. Lerchner, “Beta-VAE: Learning basic visual concepts with a constrained variational framework,” in *ICLR*, 2016. 4
- [29] R. Zhang, P. Isola, A. A. Efros, E. Shechtman, and O. Wang, “The unreasonable effectiveness of deep features as a perceptual metric,” in *CVPR*, 2018. 4
- [30] J. Song, C. Meng, and S. Ermon, “Denoising diffusion implicit models,” *arXiv preprint arXiv:2010.02502*, 2020. 4